



ISTITUTO NAZIONALE DI RICERCA METROLOGICA Repository Istituzionale

Differential readings of capacitance-based controls of attitude and displacements at the micro/nano scale

This is the author's accepted version of the contribution published as:

Original

Differential readings of capacitance-based controls of attitude and displacements at the micro/nano scale / Picotto, Gian Bartolo; Bellotti, Roberto; Sosso, Andrea. - In: MEASUREMENT SCIENCE & TECHNOLOGY. - ISSN 0957-0233. - 31:10(2020), p. 104006. [10.1088/1361-6501/ab9038]

Availability:

This version is available at: 11696/63310 since: 2020-11-13T14:57:36Z

Publisher:

IOP

Published

DOI:10.1088/1361-6501/ab9038

Terms of use:

This article is made available under terms and conditions as specified in the corresponding bibliographic description in the repository

Publisher copyright

Institute of Physics Publishing Ltd (IOP)

IOP Publishing Ltd is not responsible for any errors or omissions in this version of the manuscript or any version derived from it. The Version of Record is available online at DOI indicated above

(Article begins on next page)

ACCEPTED MANUSCRIPT

Differential readings of capacitance-based controls of attitude and displacements at the micro/nano scale

To cite this article before publication: Gian Bartolo Picotto *et al* 2020 *Meas. Sci. Technol.* in press <https://doi.org/10.1088/1361-6501/ab9038>

Manuscript version: Accepted Manuscript

Accepted Manuscript is “the version of the article accepted for publication including all changes made as a result of the peer review process, and which may also include the addition to the article by IOP Publishing of a header, an article ID, a cover sheet and/or an ‘Accepted Manuscript’ watermark, but excluding any other editing, typesetting or other changes made by IOP Publishing and/or its licensors”

This Accepted Manuscript is © 2020 IOP Publishing Ltd.

During the embargo period (the 12 month period from the publication of the Version of Record of this article), the Accepted Manuscript is fully protected by copyright and cannot be reused or reposted elsewhere.

As the Version of Record of this article is going to be / has been published on a subscription basis, this Accepted Manuscript is available for reuse under a CC BY-NC-ND 3.0 licence after the 12 month embargo period.

After the embargo period, everyone is permitted to use copy and redistribute this article for non-commercial purposes only, provided that they adhere to all the terms of the licence <https://creativecommons.org/licenses/by-nc-nd/3.0>

Although reasonable endeavours have been taken to obtain all necessary permissions from third parties to include their copyrighted content within this article, their full citation and copyright line may not be present in this Accepted Manuscript version. Before using any content from this article, please refer to the Version of Record on IOPscience once published for full citation and copyright details, as permissions will likely be required. All third party content is fully copyright protected, unless specifically stated otherwise in the figure caption in the Version of Record.

View the [article online](#) for updates and enhancements.

Differential readings of capacitance-based controls of attitude and displacements at the micro/nano scale

Gian Bartolo Picotto*, Roberto Bellotti and Andrea Sosso

Istituto Nazionale di Ricerca Metrologica, Strada delle Cacce 91, 10135 Torino, Italy

*corresponding author: g.picotto@inrim.it

Abstract

Four-quadrant plane capacitive sensors with electrodes made by thick metal plates were used in a novel configuration of a bridge-based circuit for measurement of both displacement and small angles over two axes. Their design, fabrication and testing by means of a differential set-up specifically designed is presented and discussed in terms of the measurement model, considering signal recovering, linearity, resolution and noise. Numerical calculations of the capacitors, including corrective terms for fringe effects and tilt between electrodes in a differential configuration, are developed to simulate the overall measuring system. Tests of the model were then performed that validated it by comparison with the results of displacement and small angle rotation runs traced by an interferometer and an autocollimator. Sensitivities of about 0,11 V/ μm with a $1 \cdot 10^{-3}$ relative standard deviation, and of 0,13 V/mrad with a $3 \cdot 10^{-3}$ relative standard deviation, were determined with displacements up to $\pm 50 \mu\text{m}$ and yaw rotations up to $\pm 10 \text{ mrad}$.

Keywords Capacitive Sensors, Displacements, Attitude, Differential Readings, Linearity

1. Introduction

Precise positioning and scanning at the micro and nano scales require displacement sensors that offer high linearity and resolution, to be driven by a wide bandwidth measuring electronics when operating in closed-loop controls of fast scanning systems [1,2]. Interferometers provide displacement measurements with a direct traceability to the unit of length and a high resolution by the wavelength subdivision and/or multi-pass optical paths, at the cost of some more room for optics and beam paths, namely when operating with differential optics and Abbe free set-ups.

Among others, capacitive sensors offer some advantages for displacement and attitude controls including an almost load free non-contact sensing suitable to compact assembling, thus reducing the overall metrology loop. A high dynamics and linearity of the capacitance to displacement conversion is obtained by varying the overlapping area of the counter-electrodes forming the capacitor [3] while a better sensitivity is achieved by varying the gap between the electrodes, the latter at the costs of a smaller working range [2,4]. Plane-parallel capacitive sensors with a gap variation design are widely integrated on single- or multi-axes positioning stages to be used with closed-loop controls of displacements up to several hundreds of micrometers. Either linear or differential set-ups of sensors are used on demand of the DOFs under control, accuracy specifications and somewhat mechanical constraints [1,2,9].

Sensors with plane-parallel electrodes suffer from the stray capacitance due to edge effects, flatness and roughness of the electrode's surfaces and from the unwanted out-of-parallelism between the electrodes. All these effects were deeply investigated by analytical, topological and numerical (FEM) early studies [4-8 and references therein]. The edge effects are greatly reduced by a guard-ring electrode driven at the same potential of the active electrode, thus providing a guard field surrounding the region between active and counter-electrodes [4]. On the other hand, the high sensitivity to rotations in a plane-parallel capacitor was successfully used for capacitively sensing the attitude of the moving electrode: a moving or tilting plate or optics depending on the application [2,10,11]. Furthermore, accurate measurements of small angles by plane capacitive sensors are demonstrated by a sine bar angular-to-linear displacement converter [12].

The displacements or small angle rotations to be determined by the capacitance of a plane-parallel capacitor are usually measured by electronics based on (auto-balancing) AC bridges, capacitance to voltage converters and high-impedance buffers sensing the voltage drop across the capacitor driven by a constant AC current source [2,4,9,10,13]. Other solutions include capacitance to frequency conversion, or capacitance to period conversion, charge/discharge circuits, RC phase variation [14]. The trade-off is often based on electrical/mechanical constraints, not charged moving elements, parasitic capacitances of connecting cables, available shielding and least but not last costs. Other relevant issues are the linearity of the response of the measurement circuit vs. displacement, and the electrical loading of the input circuit on the sensor. Generally, input circuits with higher loading have better linearity [4], defining another trade-off condition for the designer.

A differential set-up of plane-parallel multi-electrodes capacitive sensors designed for gap-variation measurements of translations and/or pitch and yaw rotations of a moving counter-

electrode plate is described in the sections 2 and 3, the configurations of the AC bridge for displacement and angle measurements and the model-based calculations of their deviation from linearity in section 4, the simulation of the overall electronics in section 5, the experimental and results in sections 6 and 7, and conclusions in section 8.

2. The capacitive sensors

The sensor is designed with a circular active area and a guard ring forming a three-terminal capacitor for reducing the edge effects. The active electrode is subdivided into four adjacent quadrants with the same area and electrically isolated from each other. The overall circular active area has a radius of 5,5 mm resulting in an area of about 24 mm² each quadrant. The sensor is made of thick brass metal plates glued by hard epoxy resin. A gap down to less than 0,1 mm is obtained between the quadrants and the circular ring. A plan-parallel thick metal plate is needed as moving counter-electrode.



Figure 1. The four-quadrant sensor

3. The differential measurement set-up

Differential readings of displacements are always preferable [14] to minimize the effect of mechanical and thermal drifts between fixed and moving parts. This is even more important at the nanoscale where the metrology loop of instruments is much larger than the lateral sizes of their measuring volume. In addition, the simultaneous control of the displacements and attitude of the moving elements is a key issue in precise positioning and process control in nanofabrication.

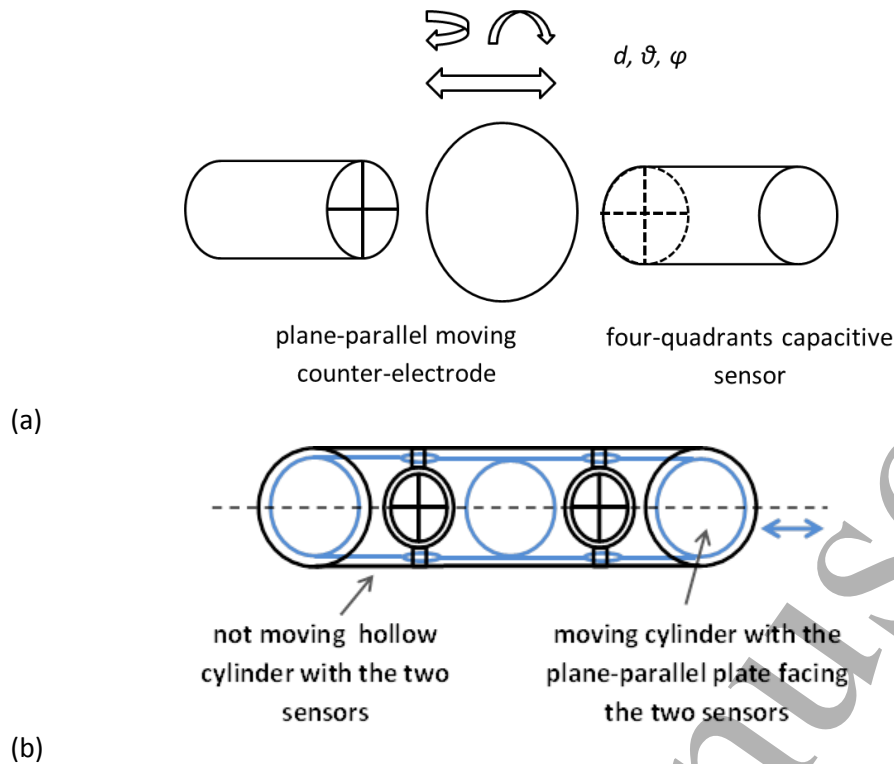


Figure 2. Sketch (a) of a differential set-up of the capacitive sensors facing a moving plane-parallel plate and a design principle (b) how to install it to monitor displacements of a moving cylinder arm.

Our differential set-up (Figure 2) consists of two four-quadrant capacitors counter-facing a plane-parallel metal plate that moves along a fixed axis of a scanning or positioning system. The translations and unwanted pitch and yaw rotations of the moving plate are detected by combining the signals from the different electrodes. In particular, the displacements summing the signals from all four quadrants, while the pitch by first summing signals of the two topmost, then taking the difference from the sum of the two in lower position, and analogously for the yaw, along the left to right direction.

The assembling of two sensors in opposition with a common mobile electrode, also called a three-plate device [4], certainly requires a more complex mechanical supports than that of a single sensor. However, for most applications where movements and pitch, yaw rotations of a mobile element are measured, the three-plate system can be effectively solved without any costs in terms of Abbe offset, as demonstrated by the design principle in Figure 2(b) of a differential device integrated in the mobile arm of a displacement actuator/transducer.

When compared to a single sensor, the advantage of a differential set-up of sensors relies on better linearity of displacements readings. Furthermore, the differential configuration would

reduce errors due to thermal drifts and geometrical effects. The advantages of a differential configuration are indeed proved by its adoption in a wide range of applications: accelerometers, position and rotation detection, force transducers, etc. [15,16].

4. Bridge-based configurations for displacements and yaw angle measurements

Two bridge-based configurations are selected and simulated for measurements of displacements and yaw rotations, respectively. For readers' convenience, the two configurations for a differential pair of semi-circle sensors are described below. The semi-circles of the two sensors are labeled as 1a, 1b and 2a, 2b respectively (Figure 3). The connection nodes A, B and C (counter electrode plate) are indicated for each semi-circle. It is worth noting that the two configurations differ from each other by different connection nodes of a pair of semi-circles.

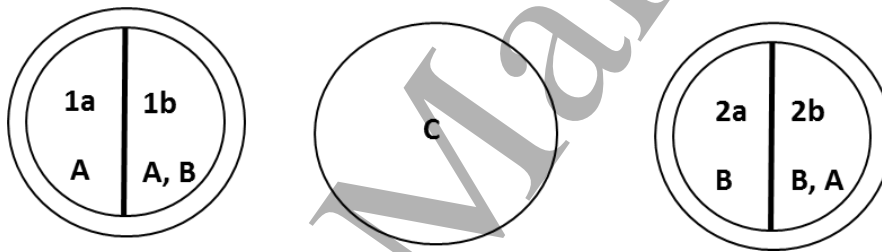


Figure 3. Two-semi-circle capacitors and the counter-electrode with their label/number and connection nodes. The surfaces of the capacitive sensors are shown as seen from the opposite counter-electrode side, i.e., '1a' is opposite to '2b', and '1b' is opposite to '2a'.

The bridge configuration for displacement measurements is shown in Figure 4(a) while that for yaw angle measurements in Figure 4(b). The transition between the two configurations takes place exchanging positions A and B of electrodes 1b and 2b, by means of a double analog switch.

The output signal at the nodes C,D named $V_{ac}(CD)$ in Figure 4, is obtained by the input V_{ac} signal at the nodes A,B ($V_{ac}(AB)$ in Figure 4) as a function of the impedances Z_1 and Z_2 in the arms of the bridge according to the equation (1):

$$V_{ac}(CD) = V_{ac}(AB) \frac{Z_1 - Z_2}{2(Z_1 + Z_2)} \quad (1)$$

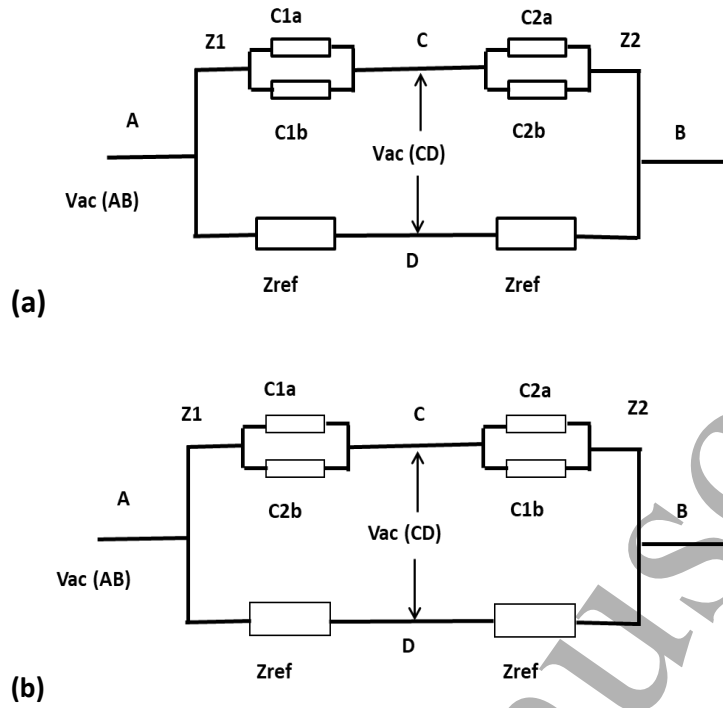
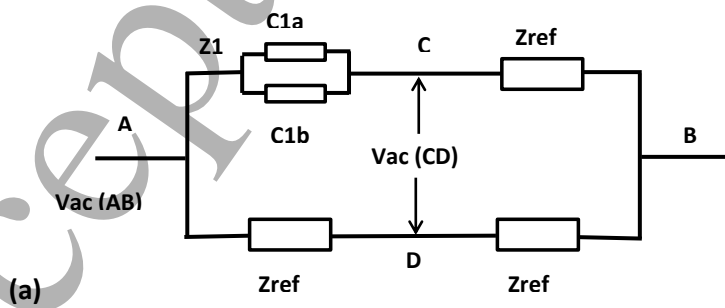


Figure 4. Bridge configurations for differential measurements of displacements (a) and yaw rotations (b).

Similarly, the bridge can be modeled for displacement and yaw rotation measurements by means of a single sensor made by two-semi-circles (Figures 5a and 5b). In this way, we can model and compare differential vs. single readings and check the effectiveness of our solution.

Considering the bridge in Figure 5b, the output signal $V_{ac}(CD)$ is given again by equation (1), while by equation (2) holds with the bridge in Figure 5a for displacements sensing.

$$V_{ac}(CD) = V_{ac}(AB) \frac{Z_1 - Z_{ref}}{2(Z_1 + Z_{ref})} \quad (2)$$



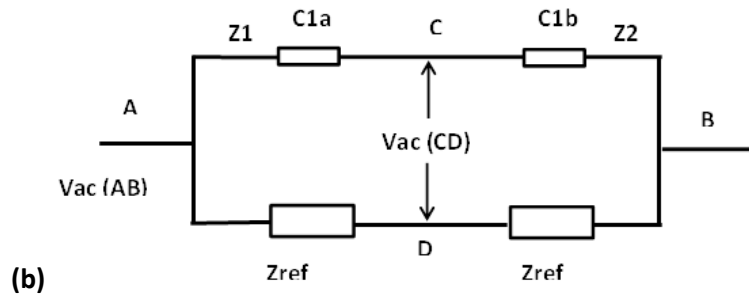


Figure 5. Bridge configurations for displacement (a) and yaw rotation (b) measurements by a two-semi-circle single sensor.

4.1 Calculation of the capacitances for a differential configuration of two-semi-circle sensors

Numerical calculations of the capacitances including corrective terms for fringe effects and deviation from parallelism between electrodes were made for a differential configuration of two-semi-circle sensors. This made it possible to identify the optimal configurations of the bridge, namely of the capacitors in the measuring arms, in order to minimize the non-linearity and optimize the sensitivity when measuring displacements and yaw rotations of a moving plane-parallel plate.

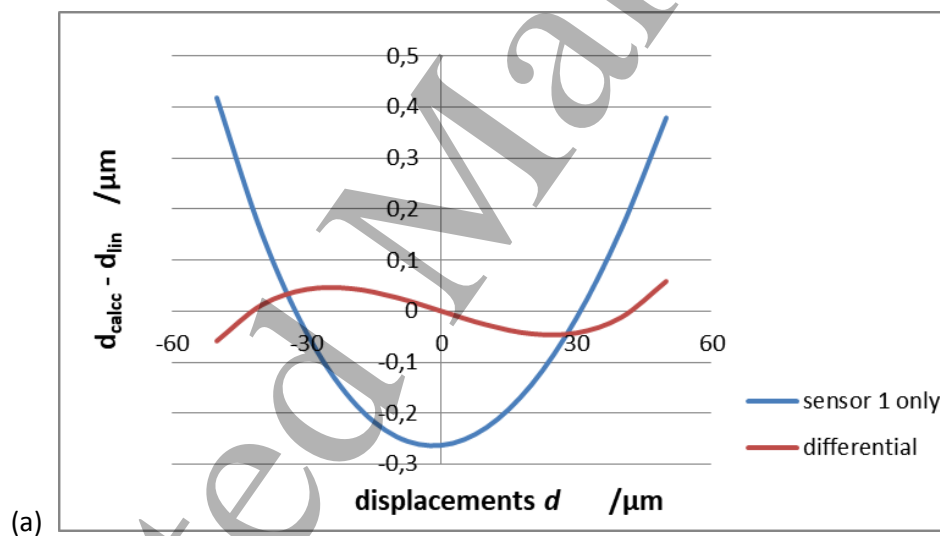
Stray capacitance due to the edge effects are calculated by the equation (3) from early works in literature [4,5 and references therein], where A is the active area, r the radius of the electrode, d the distance between electrodes, and $2\pi r$ is the length of edge.

$$C = \epsilon_r \epsilon_0 \left(\frac{A}{d} + \frac{2\pi r \ln 2}{\pi} \right) \quad (3)$$

For taking into account the capacitance changes due to small yaw angles (ϑ) between electrodes, they are calculated with the equation (4) from the reference [6].

$$C = \frac{2\epsilon_r \epsilon_0 \pi r^2}{d} \left(\frac{1}{1 + \sqrt{1 - k^2}} \right) \quad ; \quad k = \frac{r \sin 2\vartheta}{2d} \quad (4)$$

To match the mechanical constraints of a true differential assembling of sensors and a moving electrode, an initial offset and an inclination between the electrodes is assumed. Then, the deviation from linearity is determined by calculating the impedance of each capacitor independently for displacements and yaw rotations, and finally the corresponding bridge output/input ratio is obtained from equation (1) with the capacitors connected as is shown in Figures 4a or 4b. With the realistic assumption of an initial offset of 250 μm and a tilt of 5 mrad between the moving plate and the two-semi-circle sensors, a deviation from linearity of less than $1 \cdot 10^{-3}$ is determined by the differential readings, i.e., by the configuration of the bridge in Figure 4a, in a range of $\pm 50 \mu\text{m}$ displacements of the moving plate (Figure 6a), while a deviation from linearity of less than 3 % is obtained in a range of $\pm 10 \text{ mrad}$ rotations of the moving plate (Figure 6b).



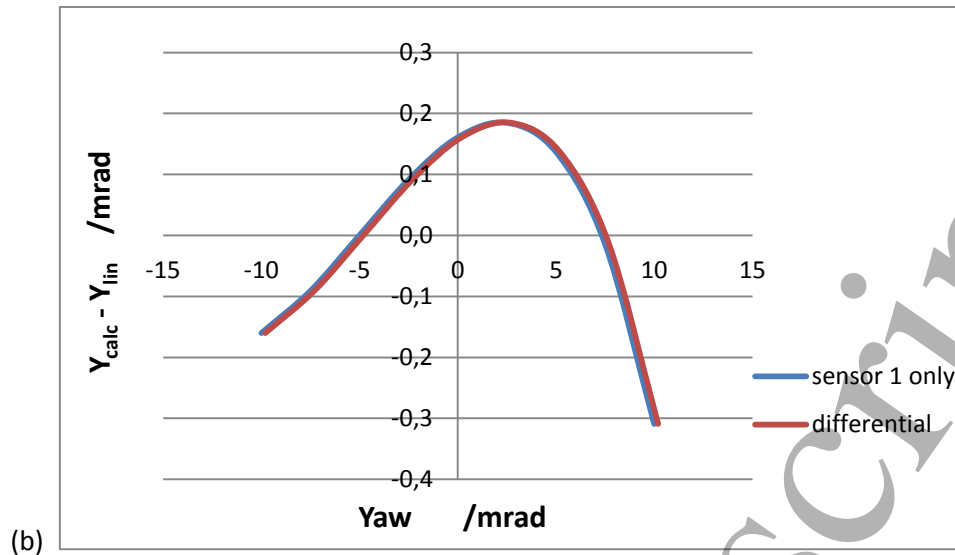


Figure 6 Calculated deviation from linearity of displacements and angle (yaw) readings by differential and single sensor configurations of the bridge.

For comparison, the readings are calculated for the bridge configurations of the differential pair and single sensor (Figures 4 and 5) and their deviation from the linearity is shown in the two graphs of Figure 6. Note that the starting position corresponds to the position at rest, i.e., at the “0” position of the outward/inward displacements of $\pm 50 \mu\text{m}$, while an initial angle between plate and electrodes is assumed to better represent a true mechanical set-up. Meanwhile, it is worth noting that a significant reduction in non-linearity is achieved with the differential readings of displacements, compared to those of the readings of a single sensor (Figure 6a). On the other side, the calculations of small angle rotations between electrodes do not show a reduction of the non-linearity between differential- to single-sensor readings. However, the differential configuration is generally preferred to minimize thermal drifts and geometric effects between mobile and fixed electrodes [4].

At this stage the calculations of yaw rotation readings do not include the geometric effect of eccentricity, precession and motions of the rotary axis combined with the thickness of the rotating plate. Assuming that a moving plate faces the active electrodes and rotates around its central vertical axis as drawn by the dense dotted lines in Figure 7, the mean distance between the electrodes and the rotating plate reduces by the amount $\Delta d = (thk/2) \cdot (1 - \cos \alpha)$, where thk is the thickness of the plate and α the rotation angle (Figure 7). Such a small decrement of the mean distance applies to all the semi-circles or quadrants of the plane electrodes, with differential or single sensor configurations.

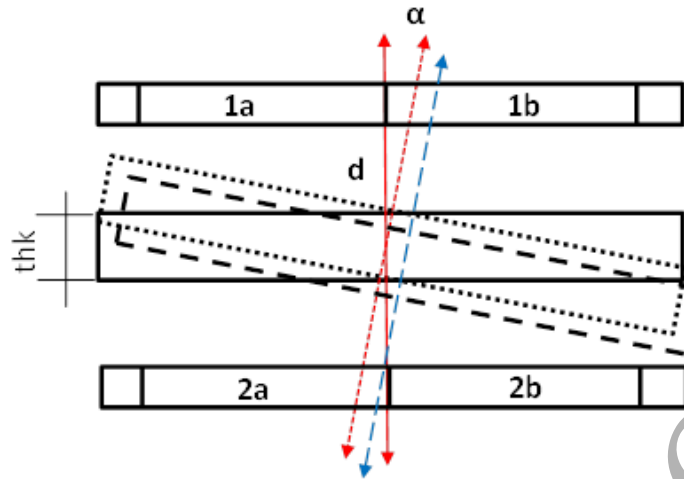


Figure 7. Sketch of a thick plate in a differential set-up of two-semi-circle sensors. Dense and sparse dotted lines represent central and eccentric yaw rotations of the plate.

This is not the case with eccentric rotations whose effects are somewhat reduced by the differential configuration. The eccentric rotation drawn by the sparse dotted lines in Figure 7 highlights the asymmetrical changes of the mean distance between the plate and the two-semi-circle sensors. However, when monitoring the yaw rotations of the moving plate the bridge is designed with the parallel of the pairs of semi-circles facing diagonally (2a-1b and 1a-2b) as drawn in Figure 4a. With an eccentric rotation, the mean distance increases for a semi-circle while decreases for the opposite-diagonal semi-circle, these two capacitors are connected in parallel in one arm of the bridge, partially compensating for such a geometric error.

5. Measurement Electronics

The electronics for testing differential capacitive sensor operation in the described set-up was specifically designed for the purpose. The basic topology of the circuit (see Figure 8) is clearly symmetric, with a balanced configuration to take the maximum advantage from the differential structure of sensors. Conversion from the single ended signal source is performed with a transformer, whose central node in the output windings is one of the measuring points. The pair of sensors is then energized by the opposite voltages at the two outer taps of transformer secondary windings in a typical bridge structure.

The selected circuit topology has the advantage that when the differential sensor is in the central position, the output signal is zero. Since the sensor is intended to operate normally with a

positioning range close to the central position, the displacement is obtained by a null measurement, with limited contributions to uncertainty from several sources, like cable loading, gain error and common mode. Additionally, the null measurement approach allows to increase arbitrarily the sensitivity of the null detector. The gain then can be set so that the full dynamic range of the detector is used over the sensor operating range. Lock-in technique allows us to increase sensitivity as needed, depending on a trade-off here between the bandwidth and the amplifier gain. The detector can then be configured according to specific measurement needs, providing very high sensitivity in quasi-static position measurement (minimum bandwidth) or fast movement monitoring (minimum gain).

Electronic switches were used to select one out of the 3 possible operating modes, as described previously: translational and rotational along y and z axes. At present, the control signal for the switches is set manually, however the circuit board is configured to for automated control, e.g. via a computer digital I/O card, to provide an almost instantaneous selection of the translational/rotational displacement to be observed. It should be noted that the electronic switches introduce an additional parasitic capacitance, whose value is very low, but may be not negligible compared to the values of the sensors in some situations. The structure of the circuit we adopted is particularly advantageous in reducing the effect of this unwanted parasitics since, as one can see in Figure 8, all currents flowing through the switches parasitic capacitance to ground has negligible effect because leakage currents come from a voltage (very low impedance) source.

The center of the capacitive sensors bridge is then taken as output signal, with the central tap of the transformer as reference node, then sent to the lock-in input to detect the bridge unbalance that provides the displacement value. The connection to the lock-in requires a cable, whose length can be limited as much as possible, but unavoidably adds an additional capacitance to ground, loading the bridge output. To reduce this detrimental loading on the high impedance output node, the current input of the lock-in was used, instead of the usual voltage input. In the case of current input, an additional current to voltage converter is present in the instrument front end, whose effect is to reduce the input voltage to a negligible value, virtually "shorting" the input, by the, so called, virtual ground action. The detection of the bridge unbalance with a current instead of voltage monitor signal then reduces the cable load to a very low level, so that it can be neglected. As the effect of cable capacitance is more relevant at low capacitance values, the elimination of cable loading effect cancels out this additive error that depends on sensor position in a way that is difficultly predictable.

In our tests the excitation signal was a 0.5 V_{pp}, 85 kHz sinewave, selected as a good compromise to reduce the sensor impedance to a manageable value, yet avoiding a significant increment in the complexity of the measurement circuit. The amplitude of the stimulus allow us to use the lock-in with a low gain (500 nA) and, soft post-detection filtering (300 ms), suited reading of both static and dynamic conditions at low speeds.

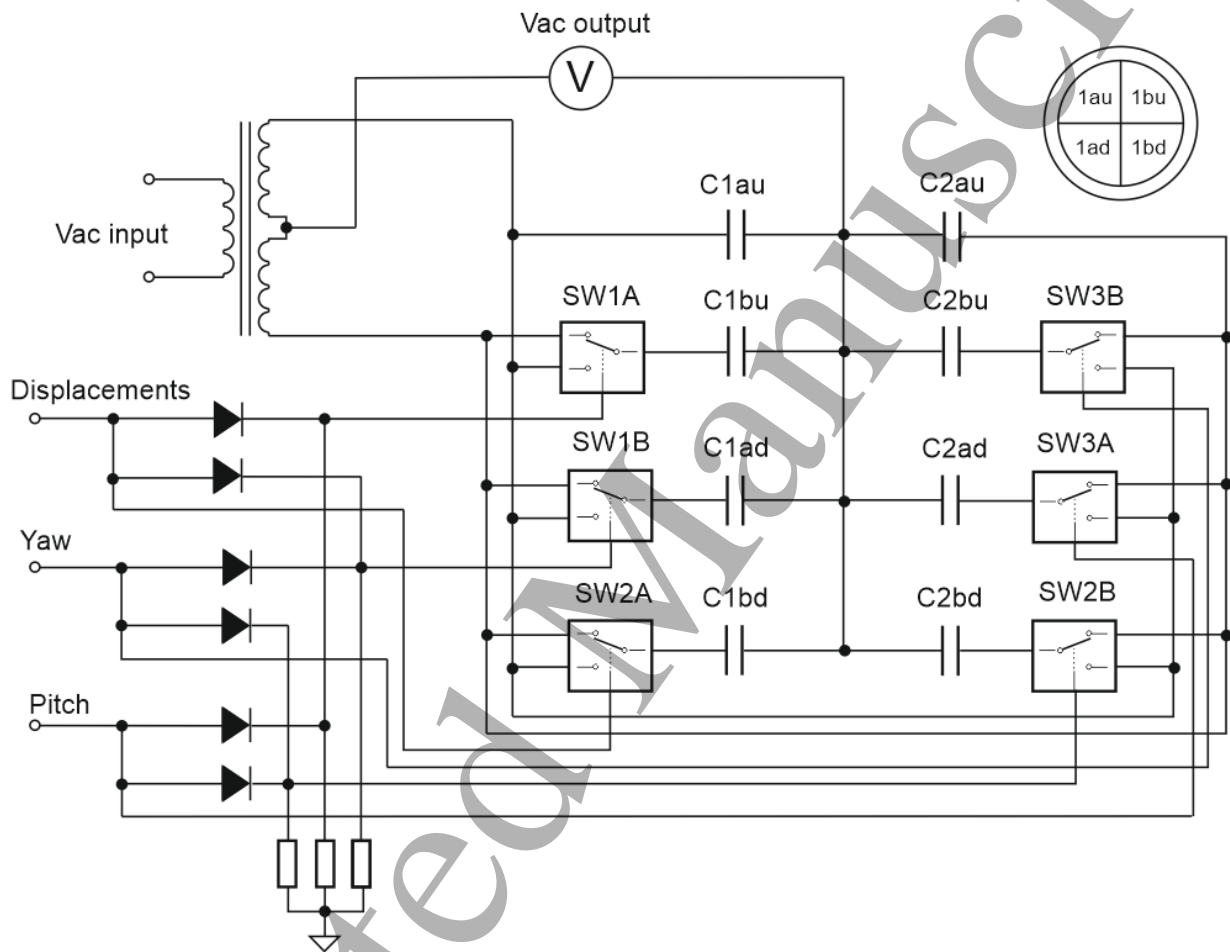


Figure 8. Schematic representation of the transformer circuit used to energize the differential capacitive sensor bridge with a balanced signal. The capacitors (C1XX and C2XX) represent the four-quadrant sensor in the upper-right side of the figure, of the two capacitive sensors facing the moving plate, i.e., the counter-electrode. The switches SWXX (ADG1236 dual switch) allow for setting the bridge to translational or axial (y,z) operating mode.

5.1 Simulation

The bridge-based configurations for displacements and angle measurements were simulated by the TI software tool (Tina-TI V9) and the circuit drawn in Figure 9 with the capacitors of a pair of two-semi-circle sensors.

Two analog switch SPICE models are used to simulate the commutations from displacements to angle readings. The switch parasitic effects are represented by series resistances (R_{sw}) and capacitances to ground (C_{on} and C_{off}) as given by the model of the commercial switch in use.

Besides, the capacitors (C_{1ab} and C_{2ab}) are introduced into the circuit to account for the parasitic capacitance between the two adjacent semi-circles of each thick-plate sensor.

By applying an AC voltage source and driving the circuit at a 100 kHz signal, we obtained the bridge output signal according to the values of the capacitors (C_{1a} , C_{1b} , C_{2a} , and C_{2b}) representing the capacitances of the differential set-up of the two-sector sensors. It is worth noting that these values are the same as those calculated in section 4.1, both for small angles and displacements between the electrodes and the moving plate. Then, the output signal of the bridge is derived by inserting into the circuit the values of the capacitors calculated according to the equations (3) and (4) to take into account displacements and yaw rotations in the ranges of the $\pm 50 \mu\text{m}$ and of $\pm 10 \text{ mrad}$, with which a deviation from linearity of about $3 \cdot 10^{-3}$ for displacements, and of 2,5 % for yaw rotations, is determined from the simulated bridge circuit.

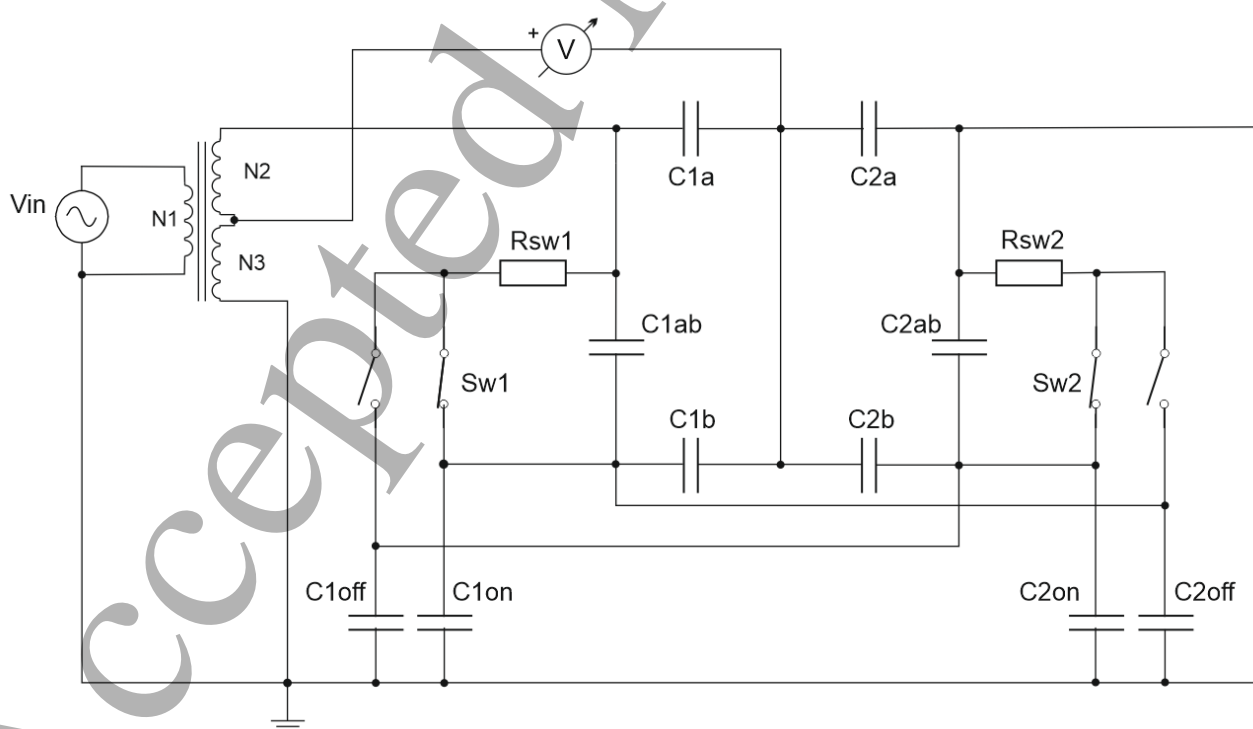
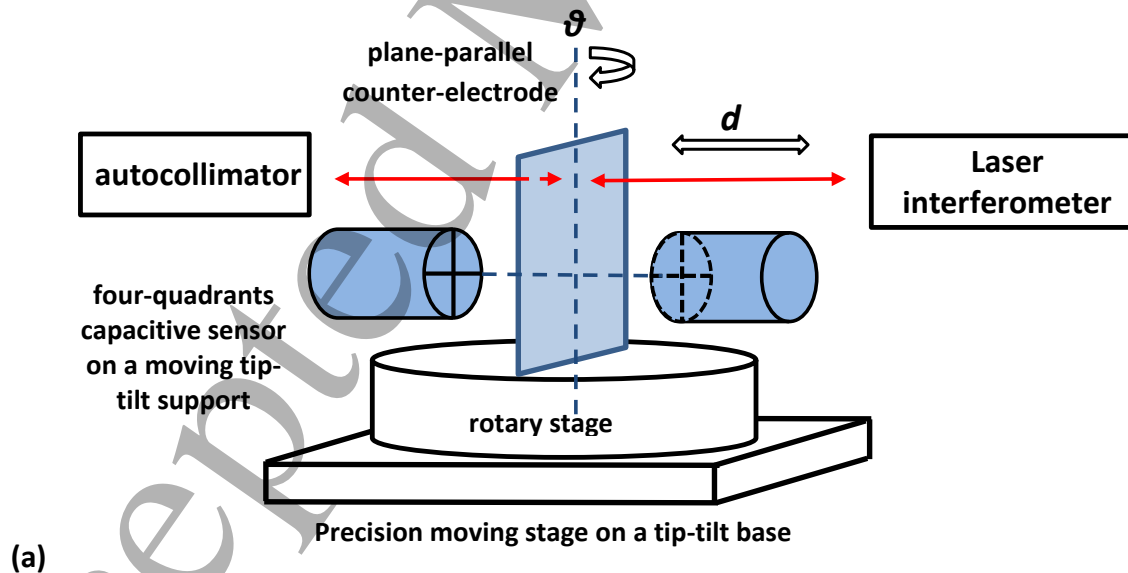


Figure 9. Schematic representation of the circuit for simulating the behavior of the bridge with a differential pair of capacitive sensors made of two sectors/electrodes (C1a, C1b, C2a, C2b). C1ab and C2ab represent the parasitic capacitors between the two adjacent thick electrodes of each sensor, while Rsw, Con and Coff represent the series resistance and the capacitances to ground of the switches.

6. Experimental

An extensive test of a differential pairs of four-quadrant capacitive sensors was performed using tip-tilt and linear stages guiding the plane-parallel moving plate, with movements and inclinations independently measured by a laser interferometer and an autocollimator (Figure 10), traceable to primary standards. Due to mechanical constraints, a vertical Abbe offset is present between the measuring axis of the capacitive sensors and the axis of the laser interferometer. However, unwanted pitch and yaw rotations of a few arcseconds of the moving plate were monitored by the autocollimator during outward and inward displacement paths up to a hundred micrometres. The moving plate is mounted in the center of the rotary table to minimize the eccentricity and precession of its central vertical axis along the rotations of the table. An unwanted coupling of about 1 % between pitch and yaw rotations was monitored when the plate was rotated in yaw in an interval up to ± 15 mrad.



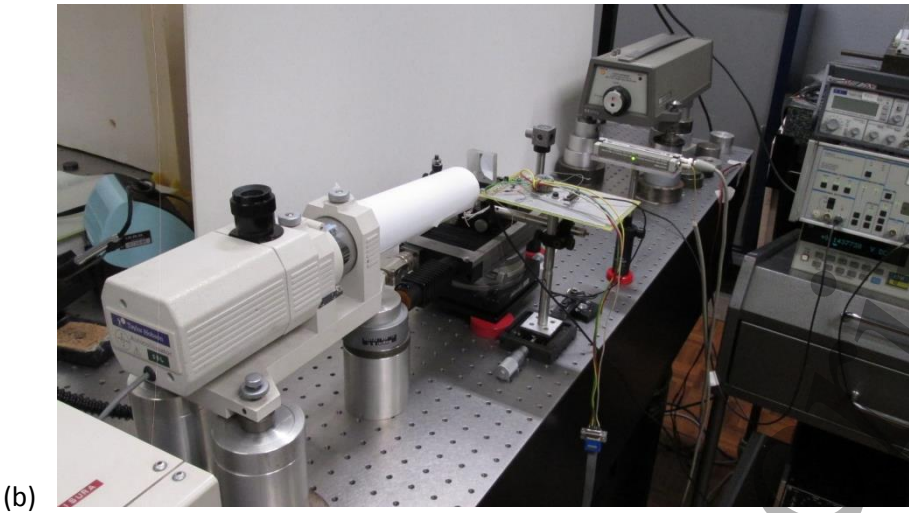


Figure 10. Sketch (a) and lateral view (b) of the apparatus to test the differential set-up of capacitive sensors.

It is worth noting that the mechanical set-up makes use of rather massive stages with bases and supports independent of the two capacitive sensors and the moving plate, all at the expense of a rather long metrology loop and of a higher sensitivity to mechanical vibrations. Significant components at frequencies up to a few hundred Hertz are present in the noise spectrum, as shown in the PSD plot of the measuring signal, namely the lock-in output signal (Figure 11). A noise of about $1 \text{ mV}/\sqrt{\text{Hz}}$ is calculated at 1 Hz with a full range 10 V output signal.

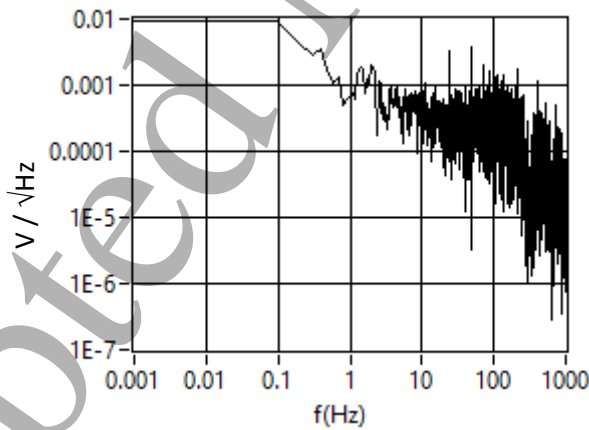


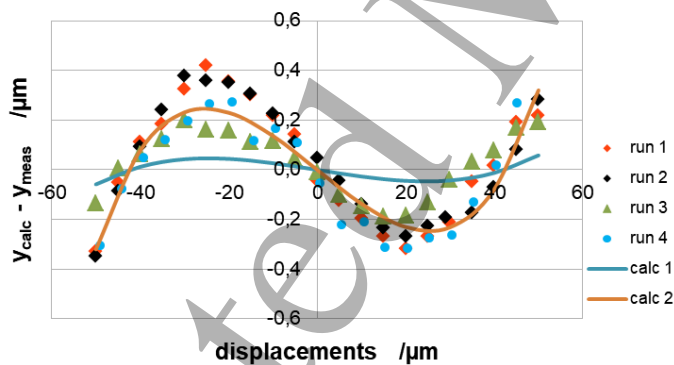
Figure 11. Power Spectral Density plot of the lock-in output signal.

7. Results

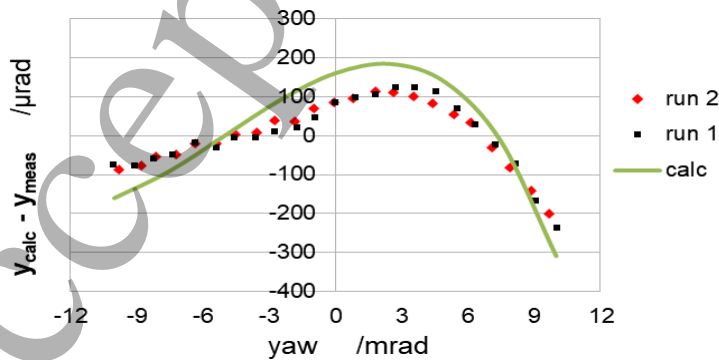
Several runs varying displacements and small rotations of the moving plate were performed by independently piloting the rotary and linear stages. Displacements and yaw rotations were

determined by measuring the DC output signal of the lock-in driven by the AC output signal of the bridge working in the configurations described in section 4. Main results are summarized by the two graphs in Figure 12. Deviation from linearity of single runs are plotted together with those calculated using the model of the bridge output in section 4.1. Among other, the calculated and measured values show a similar trend with somewhat different amplitudes. With yaw rotations, the calculated values are those shown in the plots of Figure 6, while with displacements two plots are calculated (calc1 and calc2; continuous lines) assuming different initial distances between the sensors and the moving plate, namely $250\text{ }\mu\text{m}$ with calc1 and $170\text{ }\mu\text{m}$ with calc2. As expected, a shorter initial mean distance allows for a higher sensitivity but at the cost of a larger deviation from linearity. Furthermore, we can deduce that the observed discrepancies between independent measurement runs, as well as between these and those calculated, is largely due to a different initial distance between the electrodes and the central moving plate.

Sensitivities of about $0,11\text{ V}/\mu\text{m}$ with a $1\cdot 10^{-3}$ relative standard deviation, and of $0,13\text{ V}/\text{mrad}$ with a $3\cdot 10^{-3}$ relative standard deviation, were measured with displacements up to $\pm 50\text{ }\mu\text{m}$ and rotations up to $\pm 10\text{ mrad}$. Moreover, in these intervals deviations from linearity were determined up to about $3\cdot 10^{-3}$ with displacements and about 1 % with small rotations.



(a)



(b)

Figure 12 Residuals of linear regressions of displacements (a) and yaw rotations (b) from the differential capacitive measuring system *versus* the readings of the laser interferometer and of the autocollimator.

The uncertainty of sensitivity to displacements was estimated from the linear regression model and the error propagation law, that takes into account the contributions from the uncertainty of the interferometer readings including air refractivity, dead-path, cosine and Abbe offset, the uncertainty of the output voltage readings, and the uncertainty of the linear and constant terms of the linear regression. In addition to the latter two contributions, the uncertainty of sensitivity to angles was estimated, including the contributions of the autocollimator readings and unwanted pitch rotations coupled to the yaw rotations of the movable plate. Due to the rather large mechanical assembly of the present set-up, and to the non-automated reading of the instruments, the main contributions come from Abbe offset, coupling between pitch and yaw rotations, and output signal readings, therefore, an expanded relative uncertainty equal to about 2 % of the sensitivities to movements and angles was estimated, in the range of $\pm 50 \mu\text{m}$ of displacements and of $\pm 10 \text{ mrad}$ of rotations of the moving plate. Some reduction of uncertainty is expected through a fully automated and PC-controlled measurement runs.

8. Conclusions

A differential configuration of plane-parallel multi-electrode capacitive sensors developed for gap-variation measurements of translations and/or pitch, yaw rotations of a moving counter-electrode plate was designed, simulated, and tested together with the measuring electronics. Multi-electrode plane capacitive sensors made from flat and thick metal plates and a novel configuration of the measuring electrodes and of the bridge are proposed for the independent detection of displacements and small angles from different configurations of the measuring bridge, driven at 100 kHz AC signal. A current input detection of the lock-in is used to minimize the effects of parasitic capacitances, mostly due to connecting cables. The sensitivity and non-linearity calculated for the capacitors and bridge configurations comply with those determined by the experimental tests of the full measuring system, through the readings of the laser interferometer and of the autocollimator facing the moving plate, thus providing traceable measurements to the unit of length.

A significant reduction of the non-linearity of displacement measurements, as predicted by the model, is achieved by the capacitive differential readings if compared to the readings of a single

sensor. However, the differential setting does not provide a reduction in nonlinearity when measuring the unwanted pitch and yaw rotations but, on the other hand, allows to reduce the effects of geometric error due to eccentric rotations of the counter-electrode thick plate. The results achieved so far validate the proof-of-concept and the model of the measurements. However, a more compact mechanical set-up is needed that welcomes on-board the moving plate facing the two multi-electrode sensors near the measuring bridge to determine the actual noise, linearity and uncertainty of displacements and small angle measurements, with independent and combined readings.

Acknowledgments

The Authors wish to thank their colleague Mauro Franco for the machining of the four-quadrant sensors.

References

1. G. Wilkening and L. Koenders (Editor(s)), *Nanoscale Calibration Standards and Methods: Dimensional and Related Measurements in the Micro- and Nanometer Range*, Wiley-VCH, 2005
2. S. Rescia, *Precise Measurements of Small Linear and Angular Displacements with Capacitance Methods*, https://www.bnl.gov/edm/papers/Sergio_Rescia_020118.pdf, web access December 2019
3. M. Zuhair et al., *Capacitor based angle sensor*, US patent 9772174B2, Sept, 26 2017
4. L. K. Baxter, *Capacitive Sensors: Design and Applications*, Wiley-IEEE press, 1997
5. T. R. Hicks and P.D. Atherton, *The NanoPositioning Book*, Queensgate, 1997
6. Harb S.M., et al., *Tilt errors in parallel plate capacitive micrometry*, Proc. 8th Int. Prec. Eng. Seminar, 147-150, 1995
7. S. Lányi, *Analysis of linearity errors of inverse capacitance position sensors*, Meas. Sci. Technol. 9, 1757, 1998
8. S. Nihtianov, *Capacitive Sensor Surface Quality Considerations When measuring Sub-nanometer Displacement*, Proc., Electronics-ET'08, 15–18, 2008, ISSN: 1313-1842
9. G.B. Picotto, et al., *Scanning tunneling microscopy head having integrated capacitive sensors for calibration of scanner displacements*, J. Vac. Sci. Technol. B 14(2), 897-900, 1996
10. G.B. Picotto G.B., et al., *A multi-electrode plane capacitive sensor for displacement measurements and attitude controls*, Meas. Sci. Technol., 20 (8), 084011, 2009
11. R W Bowman and D F Buscher, *Low-cost capacitive sensing for precision alignment of mirrors*, Meas. Sci. Technol. 21 055201, 2010
12. X. Tan, et al., *Improved accuracy of capacitive sensor based micro-angle measurement with angular-to-linear displacement conversion*, Rev. Sci. Instrum. 88, 115104, 2017
13. Nerino R., et al., *A novel ac current source for capacitance-based displacement measurements*, IEEE Trans. on Instrum. and Meas. 46 (2), 640-643, 1997
14. P. Ramanathan et al., *Low Value Capacitance Measurements for Capacitive Sensors – A Review*, Sensors & Transducers, 148(1), 1-10, 2013
15. K. Mochizuki, K. Watanabe, T. Masuda, *A High-Accuracy High-Speed Signal Processing Circuit of Differential-Capacitance Transducers*, IEEE Trans. Instrum. Meas. 47 1244-1247, 1998

1
2
3
4
5
6
7
8
9
10
11
12
13
14
15
16
17
18
19
20
21
22
23
24
25
26
27
28
29
30
31
32
33
34
35
36
37
38
39
40
41
42
43
44
45
46
47
48
49
50
51
52
53
54
55
56
57
58
59
60

16. G. Ferri, et al., *Automatic Bridge-based Interface for Differential Capacitive Full Sensing*, Conference Paper in Procedia Engineering, Volume 168, 1585-1588, 2016

Accepted Manuscript